7-19-2023

Degradation of oligo[poly(ethylene glycol) fumarate] hydrogels through stimulus-mediated pendent group cyclization

Andrew Chung

Burak Tavsanli

Elizabeth Gillies
Western University, egillie@uwo.ca

Degradation of oligo[poly(ethylene glycol) fumarate] hydrogels through stimulus-mediated pendent group cyclization

Andrew Chung,[a] Burak Tavsanli,[a] and Elizabeth R. Gillies[a,b*]

[a] Department of Chemistry, The University of Western Ontario, London, Ontario, Canada, N6A 5B7.

[b] Department of Chemical and Biochemical Engineering, The University of Western Ontario, London, Ontario, Canada, N6A 5B9.

[*]Author to whom correspondence should be addressed: egillie@uwo.ca

Abstract

Hydrogels are of interest for a wide range of applications including drug delivery, regenerative medicine, agriculture, and personal care products. Among the water-soluble synthetic polymers that can be processed to form hydrogels, oligo[poly(ethylene glycol) fumarate] (OPF) has attracted significant attention. The degradation of OPF can be tuned to some extent based on the poly(ethylene glycol) chain length and amount of cross-linker incorporated, but the degradation is generally quite slow, occurring over several months. Here we introduce a new approach to tune and trigger the degradation of OPF. Fumarate alkenes were functionalized to introduce protected pendent amines, that after deprotection could cyclize to 6-membered lactams, thereby cleaving the polymer backbone. Using light as a model stimulus, we demonstrated that the cleavage of an *o*-nitrobenzyl carbamate protecting group led to more rapid polymer degradation. Remaining

unfunctionalized fumarates allowed the functionalized OPF to be cross-linked, forming a hydrogel. Treatment with light led to breakdown of the hydrogels, as indicated by a more than 10-fold reduction in the compressive modulus. The functionalization and stimulus-responsive cleavage mechanism should be applicable to other stimuli, providing a versatile approach to control OPF degradation for various applications.

Keywords

Hydrogel, photoresponsive, oligo[poly(ethylene glycol) fumarate], degradation

Introduction

Over the past several decades, hydrogels have garnered substantial interest across a broad range of areas including food science, personal care, agriculture, and increasingly biomedical applications such as drug delivery, cellular therapy, wound healing, and device coatings [1-3]. They are characterized by their ability to retain significant amounts of water, making them attractive for use in water-rich environments such as the human body. By tuning their network structure and cross-linking mechanism, the mechanical properties of hydrogels can be engineered to match those of native tissues [3]. Hydrogels can be prepared from synthetic polymers including poly(hydroxyethyl methacrylate) [4], polyesters [5], poly(ester amide)s [6, 7], and poly(ethylene glycol) (PEG) [8, 9], or biopolymers such as chitosan [10], alginate [11], collagen [12], or hyaluronic acid [13].

Oligo[poly(ethylene glycol) fumarate] (OPF) is one of the synthetic polymers that has been investigated for hydrogel formation. OPF hydrogels have been studied for applications such as cartilage tissue engineering [14, 15], bone repair [16-18], neural regeneration [19, 20], and drug delivery [21]. OPF can be synthesized through reaction of fumaryl chloride with PEG in the presence of a proton scavenger [22], and cross-linked using chemical methods such as ammonium

persulfate with *N*,*N*,*N'*,*N'*-tetramethylethylenediamine [23] or photo-cross-linked using a photoinitiator such as Irgacure 2959 [24]. The addition of PEG diacrylate (PEGDA) as a cross-linker reduces the cross-linking time [25]. PEG molar mass determines many of the properties of the resulting hydrogels such as the tensile and fracture moduli as well as the biodegradation time [25-28]. Degradation of OPF hydrogels occurs relatively slowly, with mass losses ranging from 14 – 28% after 12 weeks *in vitro*, depending on the PEG molar mass and PEGDA:OPF ratio [26].

To enable enhanced control over hydrogel degradation and dynamic tuning of their physical and chemical properties, photodegradable hydrogels have been developed. In an early example, PEG-based hydrogels with photochemically cleavable *o*-nitrobenzyl moieties incorporated between the cross-linking sites were prepared [29, 30]. It was demonstrated that upon irradiation with light (365 – 405 nm), hydrogel degradation occurred, resulting in a decrease in elastic modulus. As hydrogel degradation proceeded, increased spreading of human mesenchymal stem cells was observed, indicating that cell morphology could be manipulated. It was also possible to create 3D features and patterns photochemically and to direct cell migration. Photodegradable PEG-based hydrogels were also used to develop non-fouling photoresists that could present both negative and positive features [31]. In another application, photodegradation was used to release cells after they were trapped in antibody-functionalized PEG hydrogels, showing the potential of photodegradation in cell sorting [32]. The advantages of photodegradation were demonstrated for wound healing applications where irradiation of an *o*-nitrobenzyl triazole containing hydrogel with light led to the release of cells and debonding from tissues [33]. Recently, photodegradable PEG hydrogels with encapsulated stem cells engineered to express light-activated VEGF were shown to undergo changes in mechanical properties as well as VEGF production in response to light irradiation, resulting in effects on *in vitro* vascularization and *in vivo* regeneration

[34]. Furthermore, allyl sulfide hydrogels, which undergo rapid photodegradation via radical addition-fragmentation chain transfer were demonstrated to be effective matrices for repeated organoid cell passaging [35].

In addition to the direct photochemical cleavage of polymer backbones with light, other stimuli-mediated cleavage mechanisms have also been investigated [36]. For example, polymers with ketals in their backbones can be cleaved under mildly acidic conditions [37], while those with disulfides can be cleaved with reducing agents and thioketals can be cleaved with reactive oxygen species [38]. Cyclization reactions involving pendent functional groups have also been used to indirectly cleave polymer backbones. For example, *t*-butyl carbonate protected 2,4-diaminobutyric acid or 2-pyridyl disulfide protected homocysteine units were incorporated into poly(ester amide)s [39]. Removal of the protecting groups with acid or reducing agents revealed pendent amines or thiols respectively, which subsequently cyclized on the adjacent backbone esters to form 5-membered lactams or thiolactones. *o*-Nitrobenzyl carbamate-protected pendent amines were introduced to poly(DL-lactide-*co*-glycolide) resulting in deprotection and cyclization to the 5-membered lactams after irradiation with light [40]. This approach was used to prepare degradable nanoparticles. The incorporation of *o*-nitrobenzyl carbamate-protected ornithine into poly(ester amide)s allowed cyclization to the 6-membered lactam and consequent backbone cleavage in response to light [41]. Furthermore, pendent amino groups were introduced to a hydrophobic polyester containing maleic acid *via* thiol-Michael addition of *β*-amino mercaptans [42]. In the solid state, the polymers underwent thermally-induced degradation with formation of 6-membered lactams. These mechanisms of stimulus-mediated degradation are attractive, as they allow the polymer backbone to remain the same, while the stimulus required for polymer degradation can

be changed by altering only the pendent protecting group. However, to the best of our knowledge, such triggerable cyclization reactions have not been explored in the context of hydrogels.

Described here is an approach to introduce stimulus-mediated degradation properties to OPF hydrogels (Figure 1). We show that protected pendent amino groups can be introduced to OPF by thiol-Michael addition to about 50% of the fumarate alkenes and that backbone degradation can then be triggered by unmasking of the amines. A light-responsive *o*-nitrobenzyl protected group is selected due to ease of synthesis and high spatiotemporal control [43]. It is also demonstrated that the functionalized OPF can be used to prepare hydrogels and that the hydrogels undergo degradation in response to light.

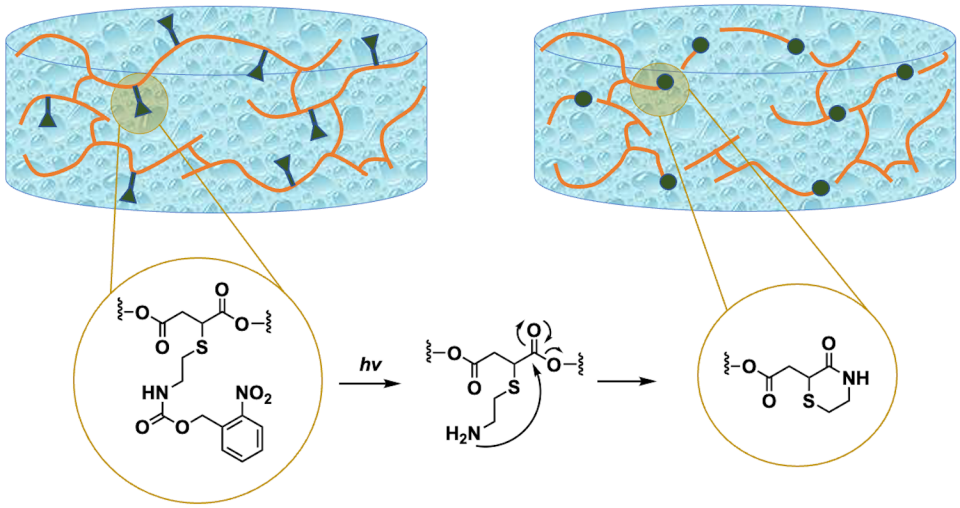

Figure 1. Schematic showing how a cross-linked hydrogel containing *o*-nitrobenzyl carbamate-functionalized amines along the polymer backbone can be triggered to cyclize, cleaving the polymer backbone, and degrading the hydrogel.

Experimental

General Materials. 2-(Tritylthio)ethanamine (**1**) [44], and 2-nitrobenzyl 4-nitrophenyl carbonate (**2**) [45] were synthesized as previously reported. Toluene, CH_3CN, CH_2Cl_2, and pyridine were purchased from Caledon Laboratory Chemicals (Georgetown, ON, Canada). Hydrochloric acid

(HCl, 12 M), triethylamine (NEt_3), poly(ethylene glycol) (M_n = 1500 g/mol) (PEG-1500), trifluoroacetic acid (TFA), cysteamine hydrochloride, trityl chloride, potassium persulfate (KPS), *N*,*N*,*N*',*N*'-tetramethylethylenediamine (TEMED), K_2CO_3, and poly(ethylene glycol) diacrylate (PEG-DA) (M_n = 575) were purchased from Sigma Aldrich (Oakville, ON, Canada). Fumaryl chloride, diethyl fumarate, and sodium hydroxide were purchased from Fisher Scientific (Hampton, NH, USA). 4-Nitrophenyl chloroformate was purchased from TCI (Montgomeryville, PA, USA). Hydroquinone was purchased from Anachemia Chemicals Ltd (Lachine, QC, Canada). All solvents and reagents were used as received unless otherwise indicated. Toluene was distilled over sodium/benzophenone under a nitrogen atmosphere before use. NEt_3 and CH_2Cl_2 were distilled over calcium hydride (CaH_2) under a nitrogen atmosphere before use. Phosphate buffered saline (PBS) was prepared to contain 137 mM NaCl, 2.7 mM KCl, 10 mM NaH_2PO_4 and 1.8 mM Na_2HPO_4.

General procedures. NMR spectra were recorded at 25 °C on a Bruker Avance HDIII 400 MHz, Bruker Neo 600 MHz, or Varian INOVA 600 MHz spectrometers. The ^1H NMR and ^{13}C NMR chemical shifts (δ) are reported in parts per million (ppm) relative to tetramethylsilane and were calibrated against the residual solvent signals of deuterated chloroform ($CHCl_3$, 7.26 ppm, 77.1 ppm) or water (HOD, 4.80 ppm). Coupling constants (J) are expressed in Hertz (Hz). Fourier-transformation infrared spectroscopy (FTIR) was performed using a PerkinElmer Spectrum Two FTIR spectrometer with an attenuated total reflectance (ATR) attachment and a single reflection diamond. The size exclusion chromatography (SEC) instrument was equipped with a Viscotek gel permeation chromatography (GPC) Max VE2001 solvent module. Samples were analyzed using the Viscotek VE3580 RI detector operating at 30 °C. The separation technique employed two Agilent Polypore (300 x 7.5 mm) columns connected in series to a Polypore guard column (50 x

7.5 mm). Samples were dissolved in chromatography grade tetrahydrofuran (THF) at approximately 5 mg/mL concentration and filtered through 0.22 μm syringe filters. Samples were injected using a 56 μL loop. The THF eluent was filtered and eluted at 1 mL/min for a total of 30 minutes. The number average molar mass (M_n), weight average molar mass (M_w), and dispersity ($Đ$) were determined relative to PEG standards with masses ranging from 400 – 106,500 g/mol. High-resolution mass spectrometry (HRMS) was conducted on a Synapt high-definition mass spectrometer using electrospray (ESI) ionization in the positive ion mode. UV-visible spectroscopy was conducted using a Cary 300 UV-visible spectrophotometer from Varian (Palo, Alto, California, USA).

Synthesis of carbamate 3. 2-Nitrobenzyl 4-nitrophenyl carbonate (**2**) (4.10 g, 12.8 mmol, 1.0 equiv) was dissolved in 150 mL of CH_3CN and then 2-(tritylthio)ethanamine (**1**) (5.35 g, 16.7 mmol, 1.3 equiv) and NEt_3 (7.2 mL, 52 mmol, 4.0 equiv) were added. The reaction mixture was stirred at room temperature overnight, and then the solvent was removed under reduced pressure and the products were redissolved in 150 mL of CH_2Cl_2. The solution was then washed with 0.5 M aqueous K_2CO_3 solution (2 x 100 mL) and brine (2 x 50 mL) and then the solvent was removed under reduced pressure to obtain an off-white solid. The crude product was recrystallized twice from 1:4 ethyl acetate:hexanes, and then washed with cold diethyl ether to provide 5.33 g of carbamate **3** as a white solid. Yield = 83%. ^{1}H NMR (400 MHz, $CDCl_3$): δ 8.09 (d, J = 9.0 Hz, 1H), 7.62-7.55 (m, 2 H), 7.49 – 7.37 (m, 7 H), 7.29 (t, J = 7.4 Hz, 6 H), 7.22 (t, J = 7.2 Hz, 3 H), 5.48 (s, 2 H), 4.90 (br s, 1 H), 3.12-2.98 (m, J = 6.3 Hz, 2 H), 2.44 (t, 6.3 Hz, 2 H). ^{13}C NMR (101 MHz, $CDCl_3$): δ 155.6, 144.7, 133.7, 133.4, 129.7, 128.8, 128.6, 128.1, 127.0, 125.1, 67.0, 63.4, 40.0, 32.4. FTIR: 3060, 1695, 1575, 1520 cm^{-1}. MS positive ion mode (m/z): calc'd for $C_{29}H_{26}N_2NaO_4S$: 521.1511; found 521.1505 $[M+Na]^+$

Synthesis of thiol 4. Carbamate **3** (5.32 g, 10.7 mmol, 1.0 equiv) was dissolved in 20 mL of anhydrous CH_2Cl_2. Triethylsilane (8.52 mL, 53.4 mmol, 5.0 equiv) was added to the solution followed by the addition of TFA (4.08 mL, 53.4 mmol, 5.0 equiv). The reaction was stirred at room temperature under argon gas for 2 h while monitoring by thin layer chromatography for completion. The TFA and CH_2Cl_2 were removed in vacuo and the crude mixture was purified by silica column chromatography (1:4 ethyl acetate:hexanes) to obtain 2.02 g of thiol **4** as an off-white solid. Yield = 74%. ^{1}H NMR (400 MHz, $CDCl_3$): δ 8.09 (d, J = 8.3 Hz, 1H), 7.67 – 7.58 (m, 2H), 7.48 (t, J = 7.6 Hz, 1H), 5.52 (s, 2H), 5.27 (br s, 1H), 3.45-3.35 (m, 2H), 2.72-2.68 (m, 2H), 1.38 (t, J = 8.5 Hz, 1). ^{13}C NMR (101 MHz, $CDCl_3$): δ 155.8, 147.6, 133.8, 133.1, 129.0, 128.8, 125.1, 63.6, 44.1, 25.0. FTIR: 2935, 1690, 1575, 1515 cm^{-1}. MS positive ion mode (m/z): calc'd for $C_{10}H_{12}N_2NaO_4S$: 279.0415; found 279.0410 $[M+Na]^+$

Synthesis of OPF. PEG-1500 was dried through azeotropic distillation using dry toluene and a Dean Stark apparatus under inert atmosphere. Fumaryl chloride was purified by distillation under Ar gas at 170 °C, and stored under Ar in the freezer until use. The PEG-1500 (20 g, 13 mmol, 1.0 equiv) was dissolved in 130 mL of dry CH_2Cl_2 with stirring and purged under Ar gas. Both distilled fumaryl chloride (1.30 mL, 12 mmol, 0.9 equiv) and anhydrous NEt_3 (3.4 mL, 24 mmol, 2.0 equiv) were each separately dissolved in 12 mL of dry CH_2Cl_2 and slowly added to the reaction using addition funnels over 2 h at 0 °C. After complete addition, the reaction mixture was stirred for 30 min at 0 °C then left to stir at 23 °C for 24 h. About 1% (w/w) of hydroquinone inhibitor (0.2 g) was then added to the mixture and the solvent was removed by rotary evaporation to obtain a brown crude product. The product was redissolved in 280 mL of ethyl acetate by heating at 40 °C for 30 min with high stirring. The salts were removed from the warm suspension by vacuum filtration and then the filtrate was cooled to 0 °C for 2 h to precipitate the product. The precipitate

was collected by vacuum filtration and then the dissolution and precipitation process was repeated. Finally, the precipitate was stirred in 1.0 L of diethyl ether, filtered, washed with diethyl ether (3 x 100 mL) and dried to give 10.8 g of OPF as a white solid. The polymer was stored under argon in the freezer until further use. Yield = 54%. ^{1}H NMR ($CDCl_3$, 400 MHz): δ 6.90 (s, 1.34 H), 4.36-4.34 (m, 3H) 3.82-3.45 (m, 136 H). ^{13}C NMR (101 MHz, $CDCl_3$): δ 164.6, 133.4, 70.3, 68.7, 64.2. FTIR: 2885, 1720. M_n = 5949 g/mol, $Đ$ =2.20.

Post-polymerization functionalization of OPF **(synthesis of *OPF-NB-100*). OPF** (400 mg, 0.17 mmol of alkene, 1.0 equiv) was dissolved in 5 mL of CH_3CN. Compound **4** (190 mg, 0.75 mmol, 4.4 equiv) was subsequently added to the reaction mixture followed by the addition of triethylamine (0.26 mL). The reaction was stirred at room temperature overnight. The solvent was removed *in vacuo* resulting in a brown solid. Diethyl ether (100 mL) was added to the crude mixture and the resulting suspension was stirred for 15 min. The precipitate was collected by vacuum filtration, washed with diethyl ether (3 x 30 mL), and dried to yield 200 mg of the product. The purified product was stored under argon in the freezer. Yield = 50 %. ^{1}H NMR (400 MHz, $CDCl_3$): δ 8.06 (d, J = 8.2 Hz, 1H), 7.66-7.59 (m, 2H), 7.46 (t, J = 7.1 Hz, 1H), 5.89 (br s, 1H), 5.50 (s, 2H), 4.41-4.18 (m, 4H), 3.81-3.40 (m, 136H), 3.02 -2.67 (m, 4H). ^{13}C NMR: δ 171.8, 170.7, 160.0, 133.9, 128.9, 128.6, 125.1, 72.7, 70.6, 68.9, 64.6, 64.3, 63.3, 61.8, 41.1, 40.2, 36.2, 32.2. FT-IR: 3411, 2884, 1960, 1729 cm^{-1}. M_n = 6164 g/mol, $Đ$ = 1.95.

Synthesis of OPF-NB-50. This polymer was synthesized by the same procedure used for the synthesis of OPF-NB-100 except that 20 mg (0.08 mmol of alkene, 0.5 eq) of compound **4** was used to provide 280 mg of product. Yield = 67%. ^{1}H NMR (400 MHz, $CDCl_3$): δ 8.07 (d, J = 8.1 Hz, 0.24 H), 7.68 – 7.54 (m, 0.54 H), 7.46 (t, J = 7.9 Hz, 0.28 H), 6.88 (s, 0.76 H), 5.88 (s, 0.28 H), 5.50 (s, 0.67 H), 4.43 – 4.28 (m, 2.48 H), 4.24 - 4.18 (m, 1.39 H), 3.89 – 3.35 (m, 136H), 3.07

– 2.63 (m, 4H). ^{13}C NMR: δ 164.6, 133.6, 133.5, 128.6, 128.3, 124.7, 72.4, 70.4, 68.7, 68.6, 64.2, 64.0, 63.0, 61.5, 40.8, 39.9, 36.0, 31.9. FT-IR: 3440, 2885, 1950, 1525, 1465 cm^{-1}. M_n = 6088 g/mol, $Đ$ = 2.31.

Analysis of polymer degradation. For ^{1}H NMR spectroscopy, OPF, OPF-NB-50, and OPF-NB-100 (20 mg) were dissolved separately in 0.8 mL of phosphate buffered D_2O (pH = 7.4, 0.1 M). For SEC, the polymers (40 mg) were dissolved in 0.8 mL of phosphate buffered H_2O (pH = 7.4, 0.1 M). For samples with remaining fumarate alkenes, 1% (w/w) hydroquinone was added as an inhibitor to prevent cross-linking (i.e. OPF and OPF-NB-50). Irradiated samples were placed in a photoreactor and irradiated with a diode array (wavelength: 365-370 nm, intensity: 10 mW/cm^2) for 30 min, while control samples were stored in the dark. All samples were then incubated at 37 °C for 7 days in the dark. ^{1}H NMR spectra of the D_2O solutions were obtained at various time points. For SEC, at various time points, 100 µL aliquots were removed from the H_2O solutions, lyophilized, redissolved in THF, filtered, and analyzed by SEC in THF.

Preparation of hydrogels (OPF/OPF-NB-50). Hydrogels were formulated at 30% (w/w) polymer. A 4:1 mass ratio of OPF or OPF-NB-50 (200 mg) and PEG-DA (45 µL) was dissolved in 290 µL of distilled water. TEMED (8.75 µL) was added to the mixture and the solution was stirred for 1 min. Subsequently, 0.2 M KPS (290 µL) in distilled water was added. The final concentrations of the KPS and TEMED were 0.1 M. The resulting solution was stirred for approximately 10 s in an ice bath and then transferred into a 1 mL syringe and incubated at 37 °C overnight.

Determination of the gel content, equilibrium water content (EWC), and mass swelling ratio. Measurements were performed in triplicate. The initial mass (m_i) of the hydrogel after preparation was recorded and the theoretical mass (m_t) was calculated as m_i x 0.3 based on the 30% (w/w) polymer in the formulation. The gel was then swelled in phosphate-buffered saline (PBS) for 24 h

and the swollen mass (m_s) was recorded. The gels were then immersed in distilled water for at least 24 h to remove salts and non-cross-linked materials. Finally, the swollen gel was frozen with liquid nitrogen and lyophilized to obtain the dry mass (m_d). The gel content, EWC, and mass swelling ratio were calculated using the equations 1-3 respectively:

$$Gel\ content = \frac{m_d}{m_t}\ x\ 100\% \quad (1)$$

$$EWC = \frac{m_s - m_d}{m_s}\ x\ 100\% \quad (2)$$

$$Mass\ swelling\ ratio = \frac{m_s - m_i}{m_i}\ x100\% \quad (3)$$

Hydrogel degradation analysis by ^{1}H NMR spectroscopy. Dried gels (15 mg) prepared from OPF-NB-50 or OPF-NB-100 were immersed in 800 µL of deuterated PBS and 1 µL of MeCN was added as an internal standard. The immersed gels were irradiated with a mercury lamp (12 mW/cm^2 of UVA; 10 mW/cm^2 of UVB, 2.7 mW/cm^2 of UVC, 9.6 mW/cm^2 of UVV) for 8 h and then incubated for 16 h at 37 °C. This irradiation and incubation sequence was repeated daily for 9 days. Control non-irradiated gels were incubated at 37 °C in the dark for 10 days. ^{1}H NMR spectra were obtained every 1-2 days for each sample.

Measurement of the compression moduli under unconfined compression. Gels were prepared as described above in 1 mL syringes. Cylindrical gels were then cut (height = ~6 mm; diameter = 5 mm) and equilibrated in PBS overnight. Unconfined compression tests were conducted using a UniVert system (Cellscale, Waterloo, ON, Canada) in a 37 °C PBS bath. OPF and OPF-NB-50 gels were tested using 10 N and 0.5 N load cells, respectively. To ensure a complete contact between gel and plates an initial compressive contact of 0.01 N was applied, and then the sample was compressed to 20% strain at a rate of 0.5%/s. Nominal stress was calculated by dividing the applied force by the cross-sectional area of the gels. The compressive moduli were calculated from

the slope of the linear region of the stress-strain curve between 5% and 15% strain. The UV irradiation treatment involved immersing the gels in PBS, irradiating them for 8 h using the mercury lamp (see preceding section for details), and then incubating them for 16 h at 37 °C in the dark. This irradiation and incubation sequence was repeated daily for 10 days. Control non-irradiated gels were incubated at 37 °C in the dark for 10 days. Compression testing was performed prior to treatment, at 5 days, and at 10 days. The measurements were performed on triplicate samples and the results are reported as the mean ± standard deviation.

Results and discussion

Synthesis of functionalized OPF

A thiol-functionalized light-responsive pendent group was synthesized for functionalization of the alkene moieties of OPF (**Scheme 1**). First, 2-(tritylthio)ethanamine (**1**) [44] and 2-nitrobenzyl 4-nitrophenyl carbonate (**2**) [45] were synthesized as previously reported. They were then combined in the presence of NEt_3 to provide the carbamate **3**. Finally, the trityl protecting group was removed using TFA in the presence of triethylsilane to give the thiol **4**. The new small molecules were characterized by ^{1}H and ^{13}C NMR spectroscopy, infrared spectroscopy, and high-resolution mass spectrometry to confirm their structures.

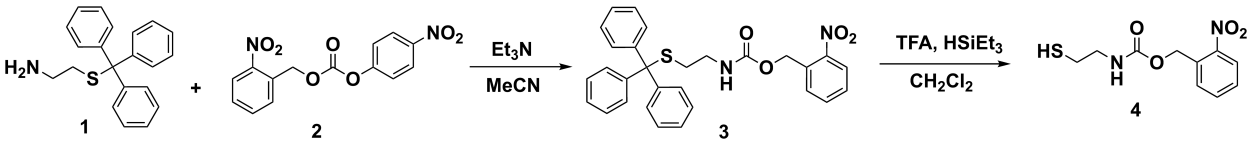

Scheme 1. Synthesis of thiol **4**.

OPF was synthesized as previously reported [22], by reaction of fumaryl chloride with PEG-1500 in dry CH_2Cl_2, except that the polymerization was run for 24 h instead of 48 h to minimize undesired cross-linking (**Scheme 2**). The yield was moderate (54%), which can likely be attributed

to the loss of some unpolymerized PEG and lower molar mass OPF during the purification process [46]. The resulting polymer had an M_n of 5950 g/mol and $Đ$ of 1.74 based on SEC in THF relative to PEG standards. ^{1}H NMR spectroscopy in $CDCl_3$ showed an intense peak at 3.64 ppm corresponding to PEG (**Figure 2a**), a peak at 4.34 ppm attributable to the methylene protons adjacent to the fumarate units, and a peak at 6.90 ppm corresponding to the fumarate alkenes. Comparison of the peak integrals for the PEG and fumarate units (Figure S5) indicated that there were about 0.7 fumarates for each PEG-1500, suggesting that the terminal units were PEG and that there were 3 – 4 PEG units per chain, in reasonable agreement with the SEC results and with those previously reported [22, 46].

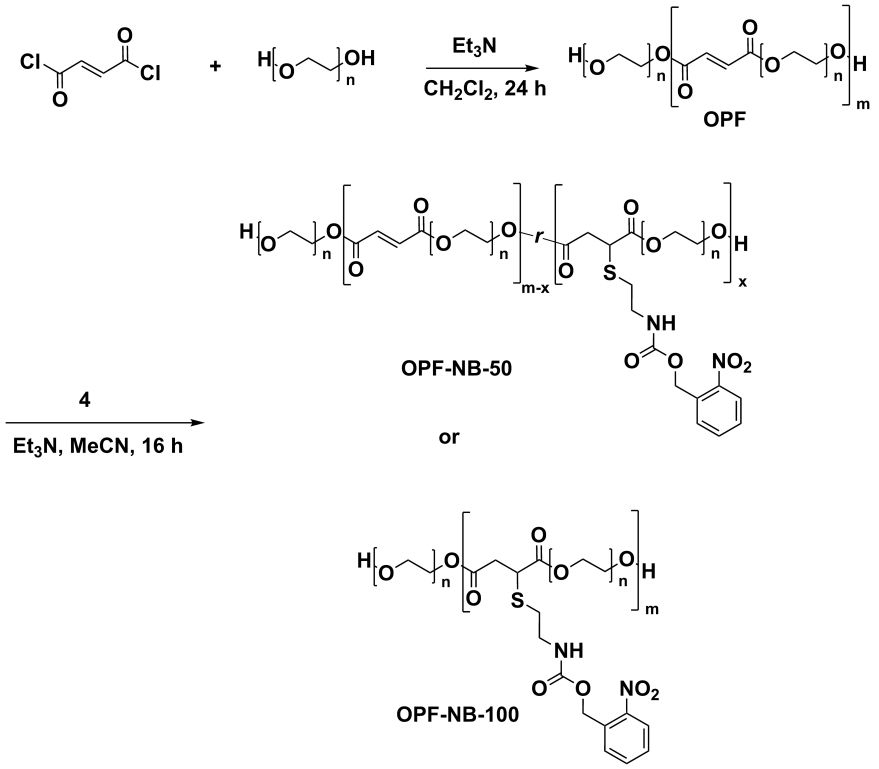

Scheme 2. Synthesis of OPF and its functionalization to provide OPF-NB-50 or OPF-NB-100.

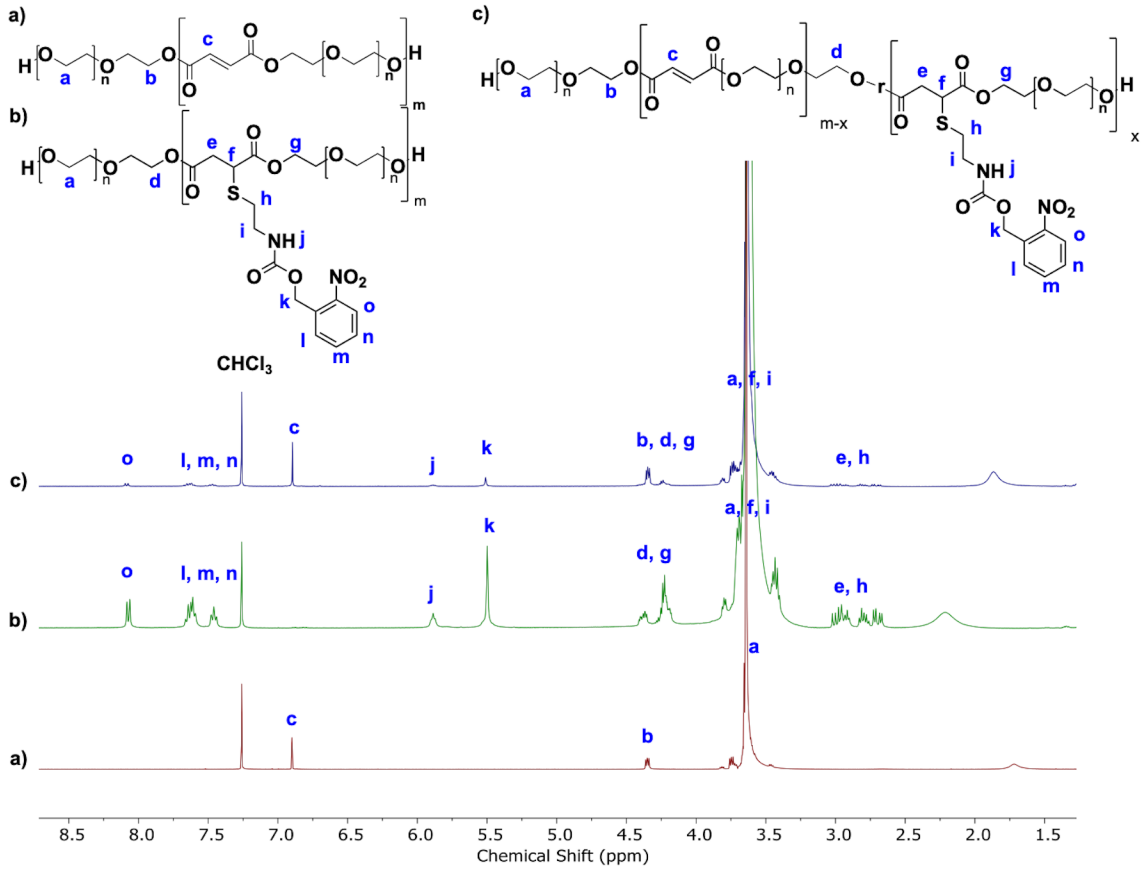

Figure 2. ^{1}H NMR spectra ($CDCl_3$, 400 MHz) of **a)** OPF, **b)** OPF-NB-100, and **c)** OPF-NB-50.

Next, the thiol **4** was reacted with OPF in the presence of NEt_3 (Scheme 2). The choice of solvent for this functionalization reaction was important. We found that although methanol resulted in a rapid thiol-Michael addition, it also led to transesterification, resulting in the breakdown of OPF. Mixtures of THF and ethanol or isopropanol resulted in slow thiol-Michael addition and incomplete functionalization [47]. On the other hand, the use of CH_3CN as the solvent allowed for full functionalization of OPF (OPF-NB-100) (**Figure 2b**), while retaining an M_n of 6164 g/mol and $Đ$ of 1.95. OPF-NB-50 was prepared by reaction with 0.5 equivalents of thiol **4** relative to the calculated moles of fumarate in the polymer, resulting in functionalization of ~45%

of the alkene peaks based on ^{1}H NMR spectroscopy (**Figure 2c, S9**). SEC indicated an M_n value of 6088 g/mol and $Đ$ of 2.31.

Degradation studies of OPF and functionalized OPF

First, ^{1}H NMR spectroscopy was used to study the degradation of OPF, OPF-NB-50, and OPF-NB-100 at 37 °C in pH 7.4 deuterated phosphate buffer (PBS-d). The inhibitor hydroquinone was added to the solutions of OPF and OPF-NB-50 to avoid undesired cross-linking of the fumarate alkenes during the experiments. When OPF was irradiated with UV light for 30 min, no significant changes in the NMR spectrum were observed. However, during incubation at 37 °C over several days, the intensity of the fumarate alkene peak at ~7.0 ppm began to decrease and two doublets appeared at 6.95 ppm and 6.53 ppm (**Figure 3a**). In addition, the peak corresponding to the methylene groups adjacent to the fumarates decreased and a new peak shifted slightly upfield emerged. These changes can likely be attributed to hydrolysis of backbone ester units. The same results were obtained for OPF that was not irradiated with UV light but was incubated in the same manner over 7 days in pH 7.4 buffer at 37 °C (Figure S11). These results confirm that hydrolysis of the backbone esters of OPF occurs, but that the rate is not impacted by UV light.

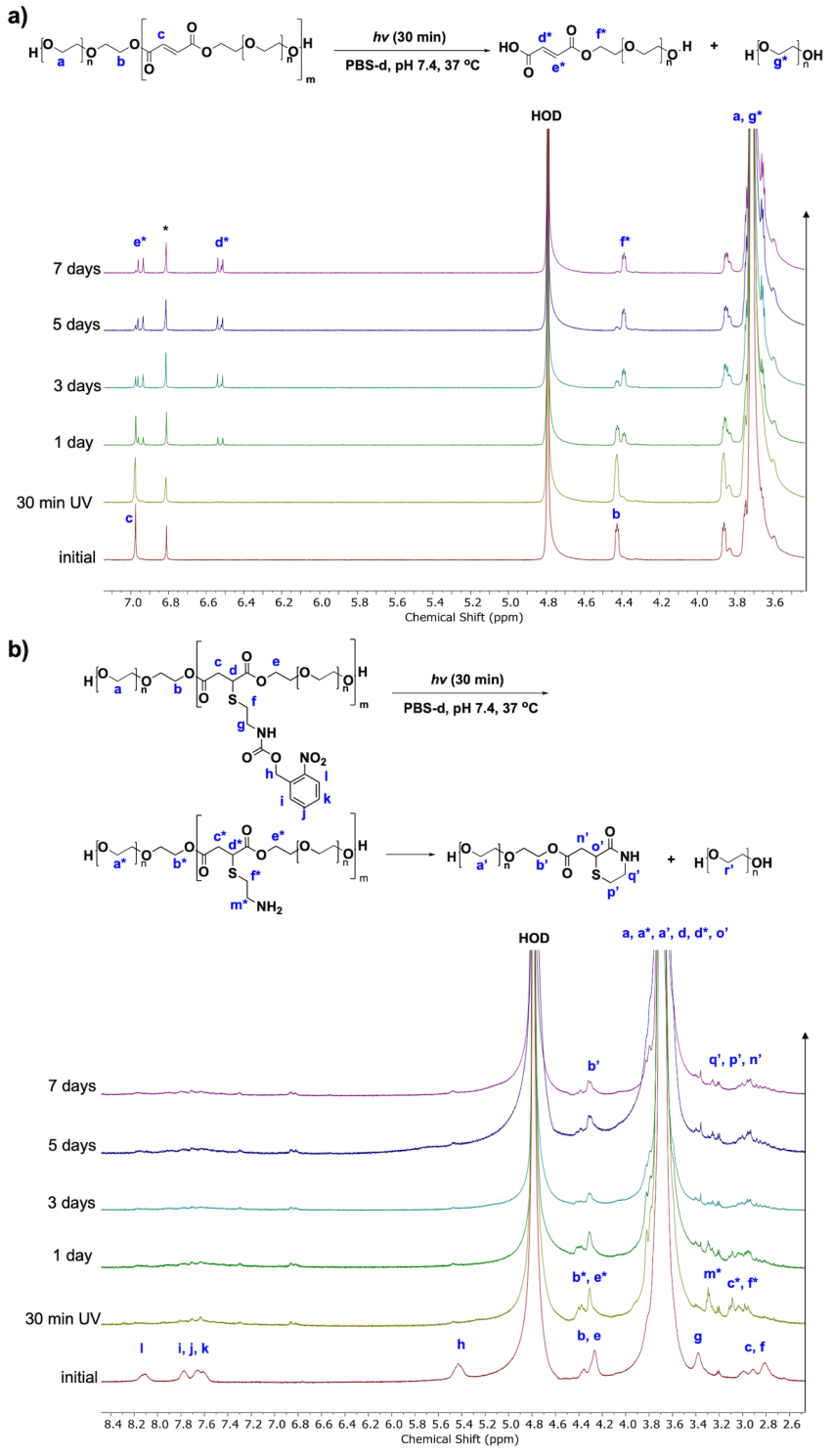

Figure 3. ^{1}H NMR spectra of a) OPF and b) OPF-NB-100 before and after irradiation with UV light and incubation at 37 °C in PBS-d (pH 7.4, 0.1 M) for various time points over 7 days. * = hydroquinone.

Next, the degradation of OPF-NB-100 was investigated. Peaks from the polymer were relatively broad, due to the fully functionalized polymer's limited solubility in PBS (**Figure 3b**). However, after irradiation with UV light for 30 min, peaks corresponding to the *o*-nitrobenzyl carbamate disappeared, with only trace peaks corresponding to the *o*-nitrobenzaldehyde byproduct and its degradation products observed in the aromatic region. Then, over the next several days there was a reduction in the intensity of the peaks from 4.4 – 4.2 ppm corresponding to the methylene groups adjacent to the ester groups, and changes in the region between 3.2 – 2.8 ppm, consistent with cyclization according to peak assignments by Lv et al. [42]. Unfortunately, the broadness of the relevant peaks and their low intensity made quantification of these changes in the NMR spectra impossible. When OPF-NB-100 was not irradiated with UV light, no significant changes in the ^{1}H NMR spectra were observed over 7 days (Figure S12). These results indicated that the rate of background ester hydrolysis for the functionalized OPF was much slower than that of OPF. The slower ester hydrolysis rate for OPF-NB-100 can likely be attributed to increased hydrophobicity and steric hindrance associated with the esters in this polymer compared with OPF. The background hydrolysis rate of OPF-NB-100 was expected to be more indicative of the background ester hydrolysis rate in OPF hydrogels, where the alkenes would be largely consumed by cross-linking and converted to esters with a saturated and branched carbon in the α position relative to the carbonyl.

The degradation of OPF-NB-50, as examined by ^{1}H NMR spectroscopy, exhibited aspects of the degradation of OPF and that of OPF-NB-100 (Figure S13-14). Peaks corresponding to the *o*-nitrobenzyl group disappeared after UV light irradiation. Subsequently, the peaks from 4.4 – 4.2 ppm corresponding to the methylene protons adjacent to the ester groups decreased in intensity.

Changes in the peaks between 3.3 – 2.7 ppm were also observed, consistent with probable cyclization. In addition, the singlet at 7.0 ppm corresponding to the remaining fumarate groups decreased in intensity, while new doublets appeared, consistent with hydrolysis of the adjacent esters. In the control experiment where OPF-NB-50 was not irradiated with UV light, the peaks corresponding to the *o*-nitrobenzyl group remained intact and no significant changes were observed in the spectrum between 3.3 – 2.7 ppm. However, the changes associated with hydrolysis adjacent to the residual fumarate groups were still observed as expected. As noted above, when incorporated into a gel, consumption of the fumarate groups during cross-linking would be expected to largely reduce the background ester hydrolysis associated with these esters.

As degradation of the polymers was difficult to quantify by ^{1}H NMR spectroscopy alone, the process was also studied by SEC. Solutions of the polymers in PBS (pH 7.4) were irradiated with UV light for 30 min, and then incubated at 37 °C for 7 days. OPF underwent an increase in peak retention time from 16 to 18 min over 7 days (**Figure 4a**), and a corresponding decrease in M_n from 5949 to 1142 g/mol (**Figure 4e**), consistent with its breakdown to release fragments similar in molar mass to the initial PEG from which it was synthesized. The M_w remained higher due to the presence of remaining oligomers. The observed changes were the same, regardless of UV light irradiation, confirming that the breakdown was due to background ester hydrolysis rather than UV-mediated degradation (**Figure 4b,e**). The irradiated OPF-NB-100 also underwent an increase in peak retention time to 18 min after 1 day, a decrease in M_n to 2100 g/mol and M_w to 4264 after 1 day, and an M_n of 1532 g/mol and M_w of 2417 after 7 days (**Figure 4c,f**). In contrast, the non-irradiated OPF-NB-100 maintained a peak retention time of 16 min for the first 3 days, with an increase to 17 min after 7 days (M_n = 2123 and M_w = 3961 g/mol) (**Figure 4d,f**). Irradiated

OPF-NB-50 also underwent an increase in the peak retention time to 18 min after 1 day (Figure S15a), with an M_n of 1731 g/mol and M_w of 2962 g/mol and M_n of 1373 g/mol and M_w of 1782 g/mol after 7 days. Non-irradiated OPG-NB-50 retained a peak retention time of 17 min until 3 days, increasing to 18 min after 7 days (Figure S15b). At 7 days, the M_n was 1614 g/mol and M_w was 2285 g/mol. Thus, despite the tendency of the esters adjacent to fumarate groups to undergo hydrolysis, these SEC results confirm that irradiation with UV light selectively accelerates degradation of the OPF functionalized *o*-nitrobenzyl protected pendent amines.

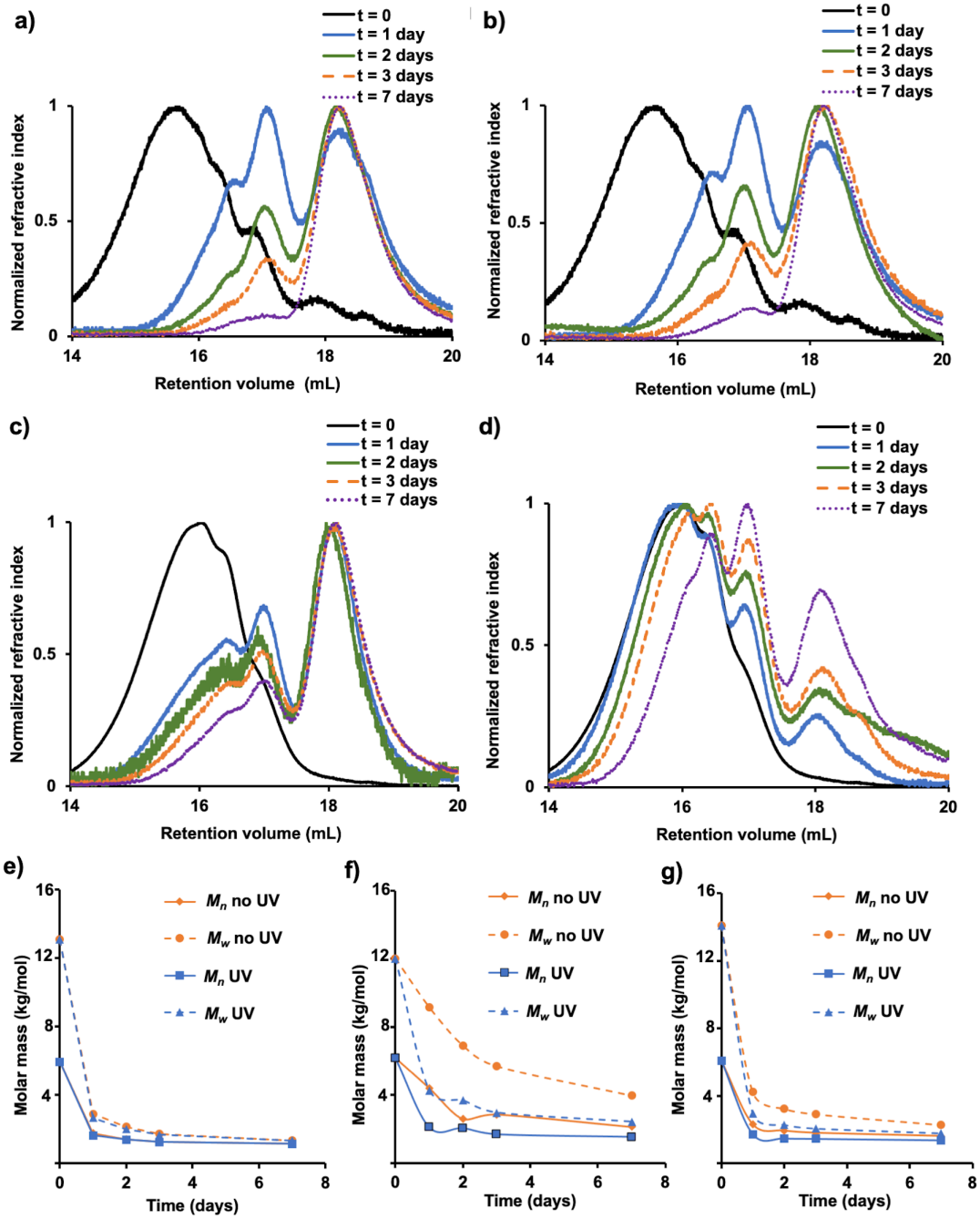

Figure 4. Analysis of degradation by SEC for polymers either irradiated with UV light for 30 min or not irradiated, followed by incubation in PBS (pH 7.4) for 7 days at 37 °C: a) OPF with UV light; b) OPF without UV light; c) OPF-NB-100 with UV light; d) OPF-NB-100 without UV light; e-g) Comparison of changes in M_n and M_w for irradiated and non-irradiated polymers: e) OPF; f) OPF-NB-50; g) OPF-NB-100.

Preparation, characterization, and degradation of hydrogels

Hydrogels were prepared from a 4:1 weight ratio of OPF or OPF-NB-50 to PEG-DA, by the addition of 0.1 M KPS and 0.1 M TEMED at 37 °C. This procedure was adapted from a previous report [48]. A formulation containing 30% (w/w) polymer was used because formulations of OPF-NB-50 at lower polymer content resulted in viscous liquids or very fragile gels. The resulting hydrogels were characterized by their gel content, EWC, mass swelling ratio, and compressive moduli as well as by SEM. The gel content for OPF-NB-50 hydrogels was substantially lower, at 47% compared to 77% for the OPF hydrogels (Table 1). This result can likely be attributed to the 2-fold lower alkene content in OPF-NB-50. Nevertheless, both the OPF and OPG-NB-50 hydrogels had very similar mass swelling ratios. At equilibrium, the OPF-NB-50 gel contained significantly more water than the OPF hydrogels, which can be attributed to the lower polymer density in the hydrogel, as reflected in the gel content. In addition, compared to the OPF hydrogel which had a compressive modulus of 164 kPa in PBS, the OPG-NB-50 hydrogel had a compressive modulus of 10 kPa, which presumably results from a substantially lower degree of cross-linking in the network. Nevertheless a modulus of 10 kPa is similar to that of soft tissues [49]. SEM of lyophilized hydrogels revealed a porous structure for the OPF-NB-50 hydrogel, whereas the OPF hydrogel appeared to be substantially less porous (**Figure 5**). It should be noted that the hydrogels likely collapse to some extent upon drying, due to the low glass transition temperature of PEG, and so caution must be used in interpreting the images of the dried hydrogels.

Table 1. Characterization of OPF and OPF-NB-50 hydrogels

Hydrogel	Gel content (%)	Mass swelling ratio (%)	EWC (%)	Compressive modulus (kPa)
OPF	77 ± 1	64 ± 1	93.0 ± 0.4	164 ± 18
OPF-NB-50	47 ± 1	63 ± 1	95.7 ± 0.2	9.6 ± 4.0

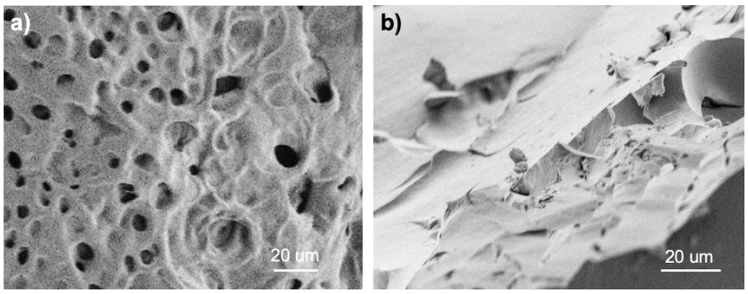

Figure 5. SEM images of lyophilized hydrogels prepared from a) OPF-NB-50 and b) OPF, suggesting a more porous structure of the OPF-NB-50 hydrogel.

The degradation of the OPF and OPG-NB-50 hydrogels was then studied by ^{1}H NMR spectroscopy. Hydrogels immersed in pH 7.4 PBS-d were irradiated with UV light for 8 h each day and incubated at 37 °C overnight. This process was repeated for 8 days. Longer irradiation times were used for these hydrogels compared to the polymer solutions as it was more difficult for the UV light to penetrate the gels. Control hydrogels were not irradiated but were incubated at 37 °C. CH_3CN was added to the samples as a reference. Before irradiation, only a low intensity broad peak was observed at 3.7 ppm for PEG, as the polymer motion was constrained in the network (**Figure 6a**). However, after irradiation, the peak became much sharper and more intense, consistent with the release of soluble PEG chains from the network. On day 8, the ratio of the PEG peak integral compared to the CH_3CN integral was 18.6:1. In contrast, for the non-irradiated OPF-

NB-50 hydrogel, the PEG peak began and remained broad, indicative of its motion remaining constrained (Figure S18). Unfortunately, the broadness of the PEG peak for this system made quantitative comparisons of peak integrals with the irradiated hydrogel problematic. OPF hydrogels also had broad, low intensity PEG peaks initially. Subsequently, regardless of irradiation, small sharp PEG peaks emerged, consistent with some release of PEG into solution (**Figure 6b**, S19). However, these peaks were much lower intensity than those observed for the irradiated OPF-NB-50 hydrogels after irradiation, reaching only an integral ratio of 3.6:1 relative to the CH_3CN peak. These results suggest that while background hydrolysis of the fumarate esters was more rapid than that of the functionalized fumarates in the NMR and SEC study of the uncross-linked polymers, once the fumarate double bond was reacted upon incorporated into the network, this background hydrolysis slowed substantially, resulting in slow background degradation of the hydrogel.

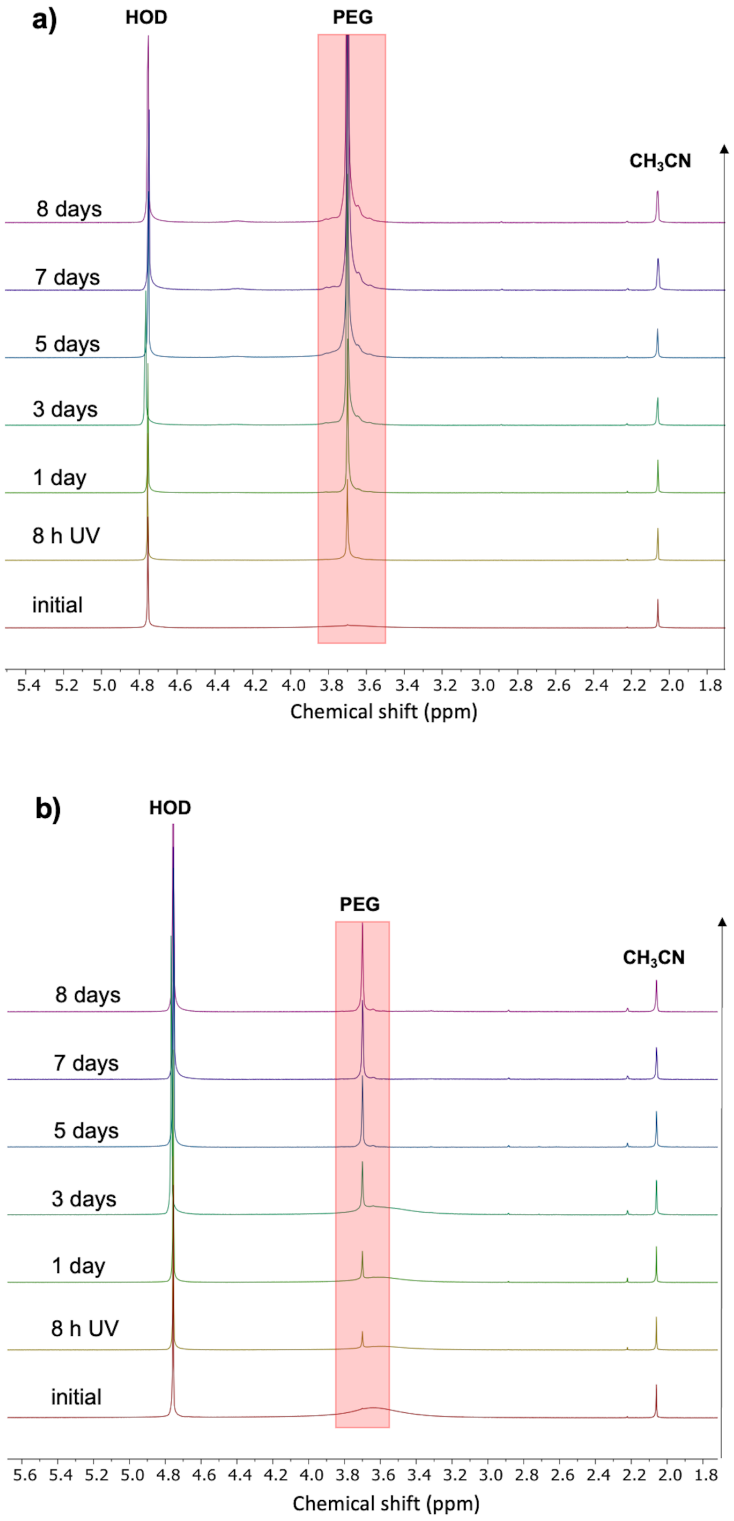

Figure 6. ^{1}H NMR spectra (600 MHz) of a) OPF-NB-50 and b) OPF hydrogels in PBS-d (pH 7.4) before UV light irradiation and after various irradiation and incubation periods. Each day of

treatment included 8 h of irradiation and 16 h at 37 °C. A larger sharp PEG peak emerged for the OPF-NB-50 hydrogel.

Hydrogel degradation was also investigated by measurements of their mechanical properties after different treatments. The compressive moduli of the hydrogels were measured initially in PBS (pH 7.4) (**Figure 7**). Then, they were irradiated with UV light for 8 h each day with incubation at 37 °C overnight over a period of 10 days, while control hydrogels were incubated in the dark at 37 °C for 10 days. Compressive moduli were measured after 5 and 10 days. Already after 5 days, the irradiated OPF-NB-50 hydrogels were too fragile and their moduli too low to be measured. This reduction in stiffness can be attributed to chemical bond cleavage and consequent breakdown of the network. On the other hand, OPF-NB-50 hydrogels that were not irradiated did not exhibit a statistically significant reduction in moduli, which remained at 8.8 ± 4.0 kPa after 5 days of incubation and 8.2 ± 3.7 kPa after 10 days. These results demonstrate that UV light leads to specific photochemically-induced cleavage rather than a dominant background hydrolysis.

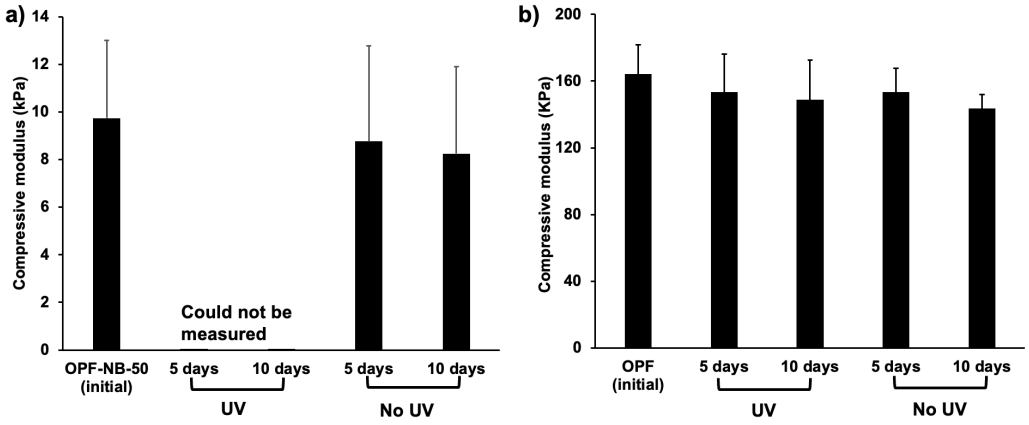

Figure 7. Compressive moduli of a) OPF-NB-50 and b) OPF hydrogels after initial preparation, swelling in PBS, and after various treatments. Irradiated samples (UV) were irradiated for 8 h

followed and incubation at 37 °C for 16 h each day for total of 10 days. The control samples (no UV) were incubated at 37 °C for the same amount of time. Error bars correspond to the standard deviation on triplicate samples. There were no statistically significant differences in moduli for the non-irradiated OPG-50-50 hydrogels or for any of the OPF hydrogels.

The degradation of the OPF networks was also examined. After 5 days of UV light irradiation and incubation, the modulus of the OPF hydrogel decreased from 164 ± 18 to 153 ± 23 kPa, and then after 10 days it was 148 ± 24 kPa. The decrease was not statistically significant, but the trend may still be indicative of a small degree of network breakdown due to ester hydrolysis. Similar decreases were observed for the control non-irradiated OPF hydrogel, the modulus of which decreased to 153 ± 14 kPa after 5 days and 143 ± 8 KPa after 10 days. These changes were also not statistically significant. It should be noted that modification of the mechanical properties of the OPF hydrogels would be more difficult compared to those of OPF-NB-50 due to the presumed higher density of cross-links in the network. Nevertheless, it was clear that only the combination of a photochemically-protected pendent group and the appropriate stimulus (i.e., UV light) led to significant changes in hydrogel mechanical properties due to triggered degradation.

Conclusions

Overall, this study demonstrated that it was possible to modulate the degradation of OPF-based hydrogels through the functionalization of OPF with pendent groups capable of cyclizing when they are revealed by a stimulus. It was challenging to demonstrate accelerated degradation of the functionalized OPF upon triggering by comparison with unfunctionalized OPF due to rapid background hydrolysis of fumarate esters. However, differences in the hydrogel degradation were

readily apparent once the more labile fumarates were consumed through cross-linking. The model stimulus employed in this work was UV light, which provides advantages such as high spatiotemporal control in the laboratory and ease of introduction of the *o*-nitrobenzyl protecting group. However, we anticipate that the chemistry can be readily expanded to impart responsiveness to near-infrared light other stimuli such as reactive oxygen species or enzymes. Such modifications would overcome the potential incompatibility of UV light with hydrogel applications involving live cells or hydrogels in vivo. An additional conclusion of this work was that consumption of the fumarate alkenes through modification with the pendent groups substantially reduced the gel content and moduli of the resulting hydrogel networks. While the reduction in stiffness may not be problematic for application of the hydrogels in soft tissues, it would be ideal to increase the gel content in future work. This might be achieved by decreasing the length of the PEG chains, thereby increasing the density of cross-linkable groups, while maintaining the density of degradation points. However, balance is required to maintain the high water-solubility of the polymers that is needed for hydrogel preparation. Overall, pendent-group modified OPF provides a promising new stimuli-responsive degradable hydrogel platform with many opportunities for further exploration.

Acknowledgments

We thank the Natural Sciences and Engineering Research Council of Canada (Discovery Grant 2021-03950) and the Canada Research Chair program (E. R. G.) for funding this work. Aneta Borecki and Zhengyu Deng are thanks for help with SEC. Xueli Mei is thanked for obtaining the SEM images.

Supporting information

^{1}H and ^{13}C NMR spectra, IR spectra, additional NMR and SEC degradation data.

Data availability

The processed data required to reproduce these findings are available to download from [insert linking to the supporting information]. Raw data is available upon request.

References

[1] S. Correa, A.K. Grosskopf, H. Lopez Hernandez, D. Chan, A.C. Yu, L.M. Stapleton, E.A. Appel, Translational applications of hydrogels, Chem. Rev. 121 (2021) 11385-11457.

[2] A. Gupta, M. Kowalczuk, W. Heaselgrave, S.T. Britland, C. Martin, I. Radecka, The production and application of hydrogels for wound management: A review, Eur. Polym. J. 111 (2019) 134-151.

[3] J. Li, X. Jia, L. Yin, Hydrogel: Diversity of structures and applications in food science, Food Rev. Int. 37 (2021) 313-372.

[4] S.J. Bryant, J.L. Cuy, K.D. Hauch, B.D. Ratner, Photo-patterning of porous hydrogels for tissue engineering, Biomaterials 28 (2007) 2978-2986.

[5] A. Basu, K.R. Kunduru, S. Doppalapudi, A. Domb, W. Khan, Poly(lactic acid) based hydrogels, Adv. Drug Delivery Rev. 107 (2016) 192-205.

[6] J. Wu, D. Wu, A. Mutschler, C.-C. Chu, Synthesis and characterization of ionic charged water soluble arginine-based poly(ester amide), J. Mater. Sci. Mater. Med. 22 (2011) 469-479.

[7] N. Liang, L.E. Flynn, E.R. Gillies, Neutral, water-soluble poly(ester amide) hydrogels for cell encapsulation, Eur. Polym. J. 136 (2020) 109899.

[8] E. Bakaic, N.M.B. Smeets, T. Hoare, Injectable hydrogels based on poly(ethylene glycol) and derivatives as functional biomaterials, RSC Adv. 5 (2015) 35469-35486.

[9] A.S. Sawhney, C.P. Pathak, J.A. Hubbell, Bioerodible hydrogels based on photopolymerized poly(ethylene glycol)-co-poly(alpha-hydroxy acid) diacrylate macromers, Macromolecules 26 (1993) 581-587.

[10] P.K. Dutta, Chitin and chitosan for regenerative medicine, Springer, Berlin, Germany, 2016.

[11] A.C. Hernandez-Gonzalez, L. Tellez-Jurado, L.M. Rodriguez-Lorenzo, Alginate hydrogels for bone tissue engineering, from injectables to bioprinting: A review, Carbohydr. Polym. 229 (2019) 115514.

[12] C. Dong, Y. Lv, Application of collagen scaffold in tissue engineering: Recent advances and new perspectives, Polymers 8 (2016) 42.

[13] C.B. Highley, G.D. Prestwich, J.A. Burdick, Recent advances in hyaluronic acid hydrogels for biomedical applications, Curr. Opin. Biotechnol. 40 (2016) 35-40.

[14] T.A. Holland, Y. Tabata, A.G. Mikos, Dual growth factor delivery from degradable oligo(poly(ethylene glycol) fumarate) hydrogel scaffolds for cartilage tissue engineering, J. Controlled Release 101 (2005) 111-125.

[15] M. Dadsetan, J.P. Szatkowski, M.J. Yaszemski, L. Lu, Characterization of photo-cross-linked oligo[poly(ethylene glycol) fumarate] hydrogels for cartilage tissue engineering, Biomacromolecules 8 (2007) 1702-1709.

[16] T.A. Holland, E.W. Bodde, L.S. Baggett, Y. Tabata, A.G. Mikos, J.A. Jansen, Osteochondral repair in the rabbit model utilizing bilayered, degradable oligo(poly(ethylene glycol) fumarate) hydrogel scaffolds, J. Biomed. Mater. Res. Part A 75 (2005) 156-167.

[17] M. Dadsetan, M. Giuliani, F. Wanivenhaus, M.B. Runge, J.E. Charlesworth, M.J. Yaszemski, Incorporation of phosphate group modulates bone cell attachment and differentiation on oligo(polyethylene glycol) fumarate hydrogel, Acta Biomater. 8 (2012) 1430-1439.
[18] M.N. George, X. Liu, A.L. Miller, H. Xu, L. Lu, Phosphate functionalization and enzymatic calcium mineralization synergistically enhance oligo[poly(ethylene glycol) fumarate] hydrogel osteoconductivity for bone tissue engineering, J. Biomed. Mater. Res. Part A 108 (2020) 515-527.
[19] M.B. Runge, M. Dadsetan, J. Baltrusaitis, T. Ruesink, L. Lu, A.J. Windebank, M.J. Yaszemski, Development of electrically conductive oligo(polyethylene glycol) fumarate-polypyrrole hydrogels for nerve regeneration, Biomacromolecules 11 (2010) 2845-2853.
[20] M. Zoughaib, K. Dayob, S. Avdokushina, M.I. Kamalov, D.V. Salakhieva, I.N. Savina, I.A. Lavrov, T.I. Abdullin, Oligo(poly(ethylene glycol) fumarate)-based multicomponent cryogels for neural tissue replacement, Gels 9 (2023) 105.
[21] T.A. Holland, Y. Tabata, A.G. Mikos, In vitro release of transforming growth factor-β1 from gelatin microparticles encapsulated in biodegradable, injectable oligo(poly(ethylene glycol) fumarate) hydrogels, J. Controlled Release 91 (2003) 299-313.
[22] L.A. Kinard, F.K. Kasper, A.G. Mikos, Synthesis of oligo(poly(ethylene glycol) fumarate), Nat. Protoc. 7 (2012) 1219-1227.
[23] J.S. Temenoff, H. Park, E. Jabbari, D.E. Conway, T.L. Sheffield, C.G. Ambrose, A.G. Mikos, Thermally cross-linked oligo(poly(ethylene glycol) fumarate) hydrogels support osteogenic differentiation of encapsulated marrow stromal cells in vitro, Biomacromolecules 5 (2004) 5-10.

[24] C.G. Williams, A.N. Malik, T.K. Kim, P.N. Manson, J.H. Elisseeff, Variable cytocompatibility of six cell lines with photoinitiators used for polymerizing hydrogels and cell encapsulation, Biomaterials 26 (2005) 1211-1218.

[25] J.S. Temenoff, K.A. Athanasiou, R.G. Lebaron, A.G. Mikos, Effect of poly(ethylene glycol) molecular weight on tensile and swelling properties of oligo(poly(ethylene glycol) fumarate) hydrogels for cartilage tissue engineering, J. Biomed. Mater. Res. Part A 59 (2002) 429-437.

[26] H. Shin, P.Q. Ruhé, A.G. Mikos, J.A. Jansen, In vivo bone and soft tissue response to injectable, biodegradable oligo(poly(ethylene glycol) fumarate) hydrogels, Biomaterials 24 (2003) 3201-3211.

[27] T.A. Holland, Y. Tabata, A.G. Mikos, In vitro release of transforming growth factor-β1 from gelatin microparticles encapsulated in biodegradable, injectable oligo(poly(ethylene glycol) fumarate) hydrogels, J. Controlled Release 91 (2003) 299-313.

[28] B. Gaihre, X. Liu, A. Lee Miller, M. Yaszemski, L. Lu, Poly(caprolactone fumarate) and oligo[poly(ethylene glycol) fumarate]: Two decades of exploration in biomedical applications, Polym. Rev. 61 (2021) 319-356.

[29] A.M. Kloxin, A.M. Kasko, C.N. Salinas, K.S. Anseth, Photodegradable hydrogels for dynamic tuning of physical and chemical properties, Science 324 (2009) 59-63.

[30] A.M. Kloxin, M.W. Tibbitt, K.S. Anseth, Synthesis of photodegradable hydrogels as dynamically tunable cell culture platforms, Nat. Protoc. 5 (2010) 1867-1887.

[31] D.Y. Wong, D.R. Griffin, J. Reed, A.M. Kasko, Photodegradable hydrogels to generate positive and negative features over multiple length scales, Macromolecules 43 (2010) 2824-2831.

[32] D.S. Shin, J. You, A. Rahimian, T. Vu, C. Siltanen, A. Ehsanipour, G. Stybayeva, J. Sutcliffe, A. Revzin, Photodegradable hydrogels for capture, detection, and release of live cells, Angew. Chem. Int. Ed. 126 (2014) 8360-8363.

[33] M. Villiou, J.I. Paez, A. Del Campo, Photodegradable hydrogels for cell encapsulation and tissue adhesion, ACS Appl. Mater. Interfaces 12 (2020) 37862-37872.

[34] E.A. Lee, S. Kim, Y. Jin, S.-W. Cho, K. Yang, N.S. Hwang, H.D. Kim, In situ microenvironment remodeling using a dual-responsive system: Photodegradable hydrogels and gene activation by visible light, Biomater. Sci. 10 (2022) 3981-3992.

[35] F.M. Yavitt, T.E. Brown, E.A. Hushka, M.E. Brown, N. Gjorevski, P.J. Dempsey, M.P. Lutolf, K.S. Anseth, The effect of thiol structure on allyl sulfide photodegradable hydrogels and their application as a degradable scaffold for organoid passaging, Adv. Mater. 32 (2020) 1905366.

[36] C. Li, Z. Deng, E.R. Gillies, Designing polymers with stimuli-responsive degradation for biomedical applications, Curr. Opin. Biomed. Eng. 25 (2022) 100437.

[37] M.J. Heffernan, N. Murthy, Polyketal nanoparticles: A new ph-sensitive biodegradable drug delivery vehicle, Bioconjugate Chem. 16 (2005) 1340-1342.

[38] M. Huo, J. Yuan, L. Tao, Y. Wei, Redox-responsive polymers for drug delivery: From molecular design to applications, Polym. Chem. 5 (2014) 1519-1528.

[39] J.S. Mejia, E.R. Gillies, Triggered degradation of poly(ester amide)s via cyclization of pendant functional groups of amino acid monomers, Polym. Chem. 4 (2013) 1969-1982.

[40] J. Olejniczak, M. Chan, A. Almutairi, Light-triggered intramolecular cyclization in poly (lactic-co-glycolic acid)-based polymers for controlled degradation, Macromolecules 48 (2015) 3166-3172.

[41] C. de Gracia Lux, J. Olejniczak, N. Fomina, M.L. Viger, A. Almutairi, Intramolecular cyclization assistance for fast degradation of ornithine-based poly(ester amide)s, J. Polym. Sci. Part A: Polym. Chem. 51 (2013) 3783-3790.

[42] A. Lv, Y. Cui, F.-S. Du, Z.-C. Li, Thermally degradable polyesters with tunable degradation temperatures via postpolymerization modification and intramolecular cyclization, Macromolecules 49 (2016) 8449-8458.

[43] J.-F. Gohy, Y. Zhao, Photo-responsive block copolymer micelles: Design and behavior, Chem. Soc. Rev. 42 (2013) 7117-7129.

[44] A.A. Watrelot, D.T. Tran, T. Buffeteau, D. Deffieux, C. Le Bourvellec, S. Quideau, C.M. Renard, Immobilization of flavan-3-ols onto sensor chips to study their interactions with proteins and pectins by SPR, Appl. Surf. Sci. 371 (2016) 512-518.

[45] T. Barra, L. Arrue, E. Urzúa, L. Ratjen, Synthesis of photocaged diamines and their application in photoinduced self-assembly, J. Phys. Org. Chem. 32 (2019) e3935.

[46] S. Jo, H. Shin, A.K. Shung, J.P. Fisher, A.G. Mikos, Synthesis and characterization of oligo(poly(ethylene glycol) fumarate) macromer, Macromolecules 34 (2001) 2839-2844.

[47] D.P. Nair, M. Podgórski, S. Chatani, T. Gong, W. Xi, C.R. Fenoli, C.N. Bowman, The thiol-michael addition click reaction: A powerful and widely used tool in materials chemistry, Chem. Mater. 26 (2013) 724-744.

[48] J.S. Temenoff, K.A. Athanasiou, R.G. LeBaron, A.G. Mikos, Effect of poly(ethylene glycol) molecular weight on tensile and swelling properties of oligo(poly(ethylene glycol) fumarate) hydrogels for cartilage tissue engineering, J. Biomed. Mater. Res. 59 (2002) 429-37.

[49] C.F. Guimarães, L. Gasperini, A.P. Marques, R.L. Reis, The stiffness of living tissues and its implications for tissue engineering, Nat. Rev. Mater. 5 (2020) 351-370.